Article

Discovery Medicine 2024; 36(186): 1464–1476
https://doi.org/10.24976/Discov.Med.202436186.136

Synergistic Effects of ^{125}I Seed Implantation Brachytherapy and Gemcitabine in Pancreatic Tumors

Qingcong Li[1], Yan Li[1], Jiayu Liu[1], Xin Huang[1], Zikang Li[1,*]

[1]Department of Oncology, Ya'an People's Hospital, 625000 Ya'an, Sichuan, China
*Correspondence: lizikanggg666@163.com (Zikang Li)
Published: 20 July 2024

Background: Monotherapy consisting of radiotherapy or chemotherapy has limited efficacy in pancreatic tumors. This study aims to investigate whether the combination of ^{125}I brachytherapy and gemcitabine (GEM) chemotherapy has a synergistic effect on pancreatic cancer (PC).

Methods: *In vitro*, PANC-1 cells in the exponential phase were treated with ^{125}I radioactive seeds (6 Gy) and GEM (30 nM). Cell proliferation, apoptosis, and mitochondrial membrane potential were measured using the Cell Counting Kit-8 (CCK-8) assay, Terminal deoxynucleotidyl transferase dUTP nick end labeling (TUNEL) staining, and flow cytometry, respectively. *In vivo*, we examined the inhibitory effect of three different treatment regimens on tumor growth in mice when combined with ^{125}I brachytherapy and GEM. Next, we investigated the effects of the optimal scheme among the three on the tumor microenvironment, tumor tissue morphology, tumor cell apoptosis, systemic inflammatory response, and levels of apoptosis-related proteins in the tumor. Changes in the tumor microenvironment and levels of apoptosis-related proteins were measured by Western blot. The extent of damage to tumor tissue morphology was assessed by Hematoxylin and Eosin (HE) staining. Tumor cell apoptosis was measured by TUNEL staining. Changes in inflammation-related factors were determined by Enzyme-Linked Immunosorbent Assay (ELISA).

Results: The results of *in vitro* cell experiments demonstrated that the combination of ^{125}I radioactive seeds (6 Gy) and GEM (30 nM) had a stronger inhibitory effect on PANC-1 cells than either alone ($p < 0.05$). *In vivo*, data showed that the GEM (after 3 d) + ^{125}I treatment group had the strongest tumor inhibition effect on PC ($p < 0.05$). Western blot analysis showed that the combined treatment of ^{125}I brachytherapy and GEM caused changes in the expression of collagen and connexin in the tumor microenvironment, promoted tumor cell apoptosis, upregulated the expression of pro-apoptotic proteins, and helped to restore pancreatic function ($p < 0.01$).

Conclusion: Our research results suggest that the strategy of ^{125}I seed implantation surgery in mice after 3 days of GEM treatment has a more pronounced synergistic effect on the treatment of PC.

Keywords: ^{125}I seed; gemcitabine; pancreatic cancer; therapy-resistance

Introduction

Pancreatic cancer (PC) is one of the most deadly cancers in clinical oncology and ranks third among causes of cancer-related death [1]. PC is inherently resistant to conventional chemotherapy due to pancreatic tumor specificity [2]. These tumors develop genetic aberrations that promote an aggressive phenotype and resistance to chemoradiotherapy [3,4]. In addition, the microenvironment of pancreatic tumors is composed of an extensive, dense, and vascular-deficient desmoplastic matrix. Together, these factors constitute a powerful barrier to drug delivery and inhibit chemoradiotherapy [5,6].

Traditionally, local pancreatic tumors are controlled by surgical resection and adjuvant chemotherapy. A previous study has shown that adjuvant therapy reduces local recurrence rates and prolongs survival [7]. In addition, neoadjuvant external-beam radiotherapy combined with surgery and chemotherapy regimens can reduce local incidence and improve overall survival [8]. Based on these results, radiation therapy combined with chemotherapy has been adopted as the first-line treatment standard for patients with advanced PC [9].

Gemcitabine (GEM), as a first-line chemotherapy drug for PC, has established efficacy in the treatment of advanced PC. However, PC patients who use GEM alone tend to develop resistance, posing some limitations to PC treatment [10]. ^{125}I seed implantation can persistently and safely kill cancer cells due to its long half-life and low-dose effect [11]. The study by Li *et al.* [12] showed that combined treatment with ^{125}I and GEM increased apoptosis in PC cells. Therefore, we speculated that the combination of ^{125}I and GEM would reduce the drug resistance of PC *in vivo*.

In our study, we first probed the inhibitory utility of ^{125}I brachytherapy combined with GEM on PC cells *in vitro*. The therapeutic effects of different regimens of ^{125}I brachytherapy and GEM combination therapy were subsequently investigated in PC xenograft mice. The mechanism of ^{125}I seed implantation after 3 days of GEM treatment against PC was further explored.

Materials and Methods

Cell Culture

We purchased a Human PC cell line (PANC-1) (iCell-h172) from iCell Bioscience Inc (Saibaikang Biotechnology Co., Ltd., Shanghai, China). The medium used for cell culture was DMEM (iCell-138-0001, Cellverse Bioscience Technology Co., Ltd., Shanghai, China) containing 10% fetal bovine serum and 1% double antibiotic. The cells were placed in air containing 5% CO_2. The incubation temperature was 37 °C. The cell lines used in this study have undergone STR profiling and tested negative for mycoplasma contamination.

Cell Intervention

Cell interventions were divided into four groups (Control group, GEM group, ^{125}I group, GEM (30 nM) + ^{125}I (6 Gy) group). We purchased ^{125}I radioactive seeds from Xinke Co., Ltd. (Shanghai, China). After PANC-1 cells had grown to the logarithmic phase, we irradiated the cells using the Gray model of ^{125}I seed radiation [13,14]. The model allows the calculation of absorbed dose and exposure time. The initial dose of radiation to PANC-1 cells was 12.13 cGy/h, and the cumulative dose was 6 Gy [15]. Drug intervention was performed by adding 100 µL of fresh complete medium containing 30 nM GEM (G8970, Solarbio, Beijing, China) to the cells [16].

Cell Counting Kit-8 (CCK-8) Assay

We cultured PANC-1 cells in 96-well plates. Then we placed PANC-1 cells in a 5% CO_2 culture environment at 37 °C. We added CCK-8 solution (Cat. No. MA0218-5, Meilunbio, Dalian, China) to the 96-well plates at a fixed time and incubated PANC-1 cells in the dark for 2 h. The absorbance of PANC-1 cell viability was detected at 450 nm by a microplate reader (Cmax plus, Molecular Devices Corporation, Silicon Valley, CA, USA). Cell viability (%) = (Absorbance of the control group – Absorbance of the blank control group)/(Absorbance of the experimental group – Absorbance of blank control group) × 100%.

Apoptosis Assay

We assessed the apoptosis of PANC-1 cells using a Terminal deoxynucleotidyl transferase dUTP nick end labeling (TUNEL) dye assay (T2130, Solarbio, Beijing, China). Simultaneously, 4′,6-Diamidino-2-phenylindole (DAPI) antibody (C0060, Solarbio, Beijing, China) was introduced to the PANC-1 cells. The apoptotic cell count in PANC-1 cells was observed through a microscope (CX53, Olympus, Tokyo, Japan).

Flow Cytometry

PANC-1 cells were seeded in 6-well plates. The cells were cultured for 12 hours. Cells were then harvested and resuspended with JC-1 dye (M8650, Solarbio, Beijing, China) at 37 °C for 30 min in the dark. Changes in mitochondrial membrane potential were quantified by flow cytometry (BECKMAN, Beckman Coulter Co., Ltd., Brea, CA, USA) using red and green fluorescence.

Mice Model of Pancreatic Cancer

Fifty female Specific Pathogen-Free (SPF) C57BL/6 mice, aged 5–6 weeks and weighing (17 ± 2) g, were purchased from the Shanghai Institute of Materia Medica, Chinese Academy of Sciences. The animals were kept in an SPF environment with a constant temperature of 22–25 °C, constant humidity of 50%–60%, natural light, and free access to food and water.

Random assignment into five groups was conducted using a random number table method. Forty mice were randomly selected. The remaining 10 serve as a non-modeled Control group. Subcutaneous injection of PANC-1 tumor cells (1×10^5 cells/mL) was performed in the left axillary region of mice to establish a PC xenograft mouse model. The PANC-1 cell suspension was adjusted to an appropriate concentration of 1×10^5 cells/mL to ensure the injection provided a specific quantity of viable cells. The health status of the mice was monitored and the growth of the tumor following the cell injection was recorded. After one week of growth, the mice were randomly divided into 4 groups (n = 10). According to the study design, mice in the experimental groups received one of 3 different treatments. To anesthetize the mice, pentobarbital sodium (30 mg/kg) was used, and the ^{125}I particles were implanted into the left axillary region of the mice using appropriate surgical techniques. Following implantation, the surgical incision was treated to ensure the mice's recovery. Mice in the first experimental group received an intravenous tail injection of GEM (50 mg/kg) for three days, followed by the implantation of ^{125}I seeds. Mice in the second group received concurrent tail vein injection of GEM (50 mg/kg) and the implantation of ^{125}I seeds. Mice in the third group received GEM (50 mg/kg) via tail vein injection three days after the implantation of ^{125}I seeds. Euthanasia was performed on mice by intravenous injection of pentobarbital sodium (110 mg/kg) through the tail vein. The study has obtained approval from the Beijing KeWeiTe for Experimental Animal Welfare Ethics Committee (Approval No. KWT-2023-084).

Tumor Growth Indicators

The specific growth of the tumor was observed, and the specific weight and volume of the tumor were counted on the 21st day. The specific size of tumor tissue was measured by the vernier caliper. Tumor volume = [(length × width)/2]^3 × 0.5236. Tumor inhibition rate = (1 – tumor volume of experimental group/tumor volume of the Control group) × 100%. After the mice were euthanized, the tumor metastasis was carefully observed and the number of metastatic lesions was counted.

HE Staining

The pancreatic tumor tissue samples were collected from the mice and fixed by adding formalin (G2161, Solarbio, Beijing, China). Samples were dehydrated by immersing them in a series of increasing concentrations of ethanol. Phenol (108-95-2, MITSUBISHI CHEMICAL GROUP, Tokyo, Japan) was added for clearing. The cleared tissue samples were immersed in molten paraffin. After paraffin embedding, the tissue samples were placed in an embedding machine (EG1150C, Leica Microsystems, Wetzlar, Germany). A rotary microtome or an ultra-thin sectioning machine (RM2255, Leica Microsystems, Wetzlar, Germany) was used to cut the tissue blocks into extremely thin sections. Sections were stained by adding hematoxylin-eosin solution (G1120, Solarbio, Beijing, China). Sections were dehydrated, cleared and mounted. Finally, we observed the stained sections under a microscope (DM5000, Leica Microsystems, Wetzlar, Germany) for pathological analysis.

Distribution of ^{125}I Radiation

The ^{125}I activity in the tumor and blood of the mice was counted using a Wallac Wizard 3 automated gamma counter (1470, Perkin Elmer, Waltham, MA, USA).

Western Blot

Proteins were separated by SDS-polyacrylamide gel electrophoresis and then transferred to a polyvinylidene fluoride (PVDF) membrane. The PVDF membrane was placed in 5% BSA at 25 °C for 1 h. Then Cleaved Caspase-3 (1:2000 dilution; cat no. ab2302, Abcam, Cambridge, UK), Cleaved Caspase-9 (1:1000 dilution; cat no. AF5240, Affinity Biosciences, Guangzhou, China), B-cell lymphoma 2 (Bcl-2) (1:2000 dilution; cat no. ab182858, Abcam, Cambridge, UK), Bcl-2–associated X protein (Bax) (1:2000 dilution; cat no. ab182733, Abcam, Cambridge, UK), Claudin-4 (1:2000 dilution; cat no. ab210796, Abcam, Cambridge, UK), Cluster of Differentiation 31 (CD-31) (1:2000 dilution; cat no. ab28364, Abcam, Cambridge, UK), Cluster of Differentiation 144 (CD-144) (1:2000 dilution; cat no. ab313632, Abcam, Cambridge, UK), and Glyceraldehyde-3-phosphate dehydrogenase (GAPDH) (1:2000 dilution; cat no. Ab9485, Abcam, Cambridge, UK) antibodies were added and incubated at 4 °C for 12 h. The PVDF membrane was then incubated with secondary antibody horseradish peroxidase (HRP) (1:2000 dilution; cat no. ZB-2305, ZB-2301, ZSGB-BIO, Beijing, China). Finally, the protein was quantitatively analyzed with a chemiluminescence enhancement kit (E-IR-R301, Elabscience Biotechnology Co., Ltd., Wuhan, China). Visualizing protein bands using gel imaging systems (Chemi-Doc MP Imaging System, Bio-Rad ChemiDoc, Hercules, CA, USA) and performing quantitative analysis of the bands using Image J software (version 1.5e, National Institutes of Health, Bethesda, MD, USA). The grey values of protein bands in this study are normalized with GAPDH as an internal reference.

Enzyme-Linked Immunosorbent Assay (ELISA)

Using a double-antibody sandwich assay, we analyzed the activity of secretory phospholipase A2 (sPLA2) (H243-2), amylase (C016-1-1), Alanine Aminotransferase (ALT) (C009-2-1), and Aspartate Aminotransferase (AST) (C010-2-1) in peripheral blood. Enzyme-Linked Immunosorbent Assay (ELISA) detection kits were purchased from Nanjing Jiancheng Biological Engineering Institute (Nanjing, China). Data were acquired using a Multiskan Go microplate reader (Cmax plus, Molecular Devices Corporation, Silicon Valley, CA, USA).

Statistical Analyses

The data were expressed as the mean ± standard deviation, and p values < 0.05 were considered significant. GraphPad Prime software 8.0 (GraphPad Prime Inc, San Diego, CA, USA, https://www.graphpad-prism.cn/) was used for statistical analysis. Data were statistically analyzed using a T-test and analysis of variance (ANOVA). Using Tukey's test for post hoc analysis.

Results

^{125}I Seeds and Gemcitabine Suppressed PANC-1 Cell Viability, Promoted Apoptosis, and Reduced Mitochondrial Membrane Potential

PANC-1 cells were irradiated with ^{125}I seeds at a dose of up to 6 Gy and treated with GEM at a dose of 30 nM. The effects of ^{125}I seeds and GEM alone and in combination on the survival rate, apoptosis, and mitochondrial membrane potential of PANC-1 cells were comprehensively evaluated.

Fig. 1A illustrates the inhibitory effect of ^{125}I seeds and GEM on the activity of PANC-1 cells. Compared with the Control group, the viability of PANC-1 cells in the GEM (30 nM) treatment group, ^{125}I (6 Gy) treatment group, and GEM (30 nM) + ^{125}I (6 Gy) combined treatment group was significantly decreased ($p < 0.05$). When ^{125}I seeds and GEM were used alone, the results showed that the inhibitory effect of ^{125}I seeds on the viability of PC cells was significantly lower than that of GEM ($p < 0.05$). Notably, the in-

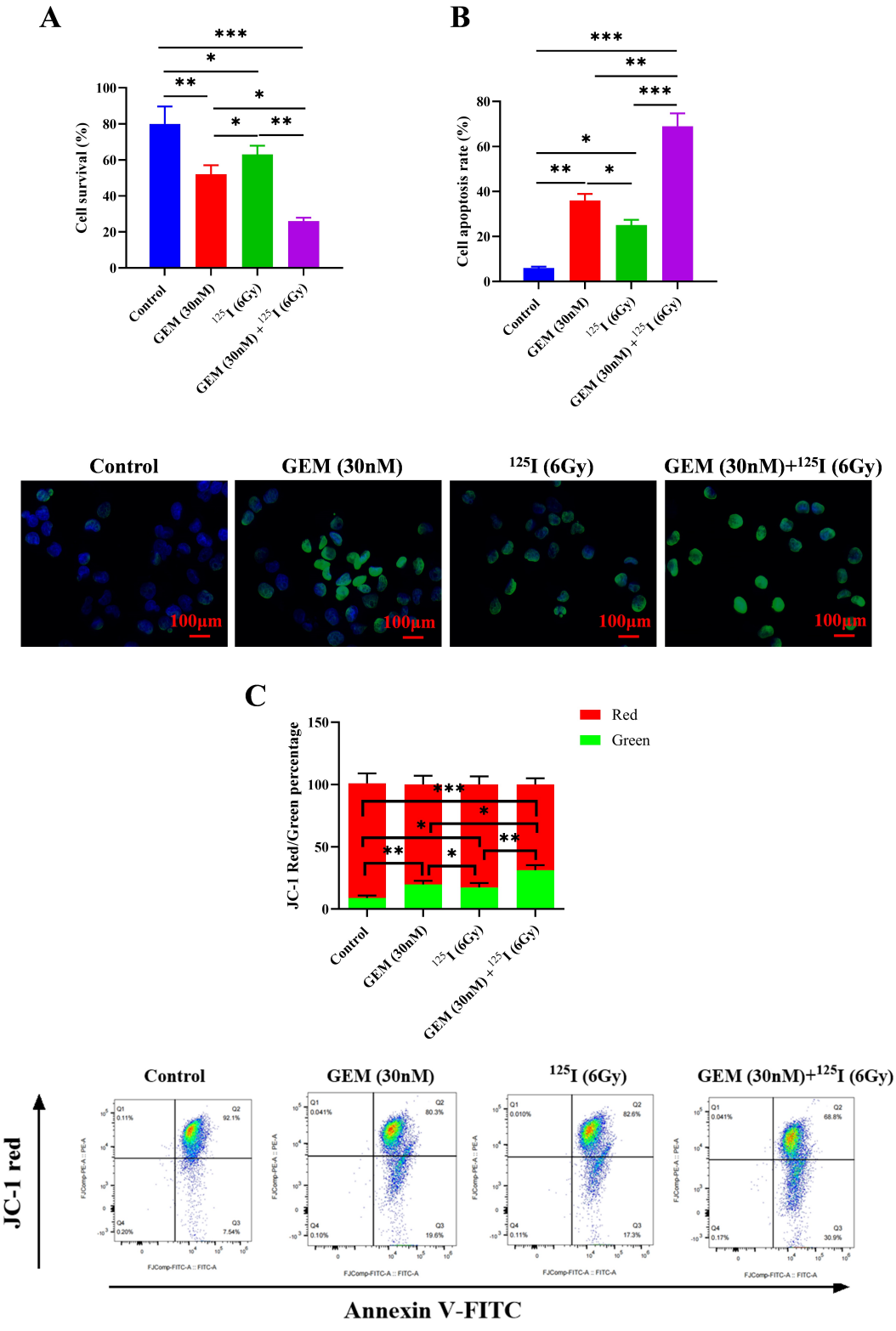

Fig. 1. Effects of ^{125}I radioactive seeds and gemcitabine on cell viability, apoptosis, and mitochondrial membrane potential of PANC-1 cells. (A) Effect of ^{125}I seeds, GEM, and GEM + ^{125}I on PANC-1 cell viability. (B) Effect of ^{125}I seeds, GEM, and GEM + ^{125}I on PANC-1 cell apoptosis. Scale bar: 100 μm. Green: Expression level of the apoptosis marker protein labeled with GFP; Blue: Cell nuclei labeled with DAPI. (C) Effect of ^{125}I seeds, GEM, and GEM + ^{125}I on PANC-1 cell mitochondrial membrane potential. (n = 6) (*$p < 0.05$, **$p < 0.01$, ***$p < 0.001$). GEM, gemcitabine; GFP, green fluorescent protein; DAPI, 4′,6-diamidino-2-phenylindole.

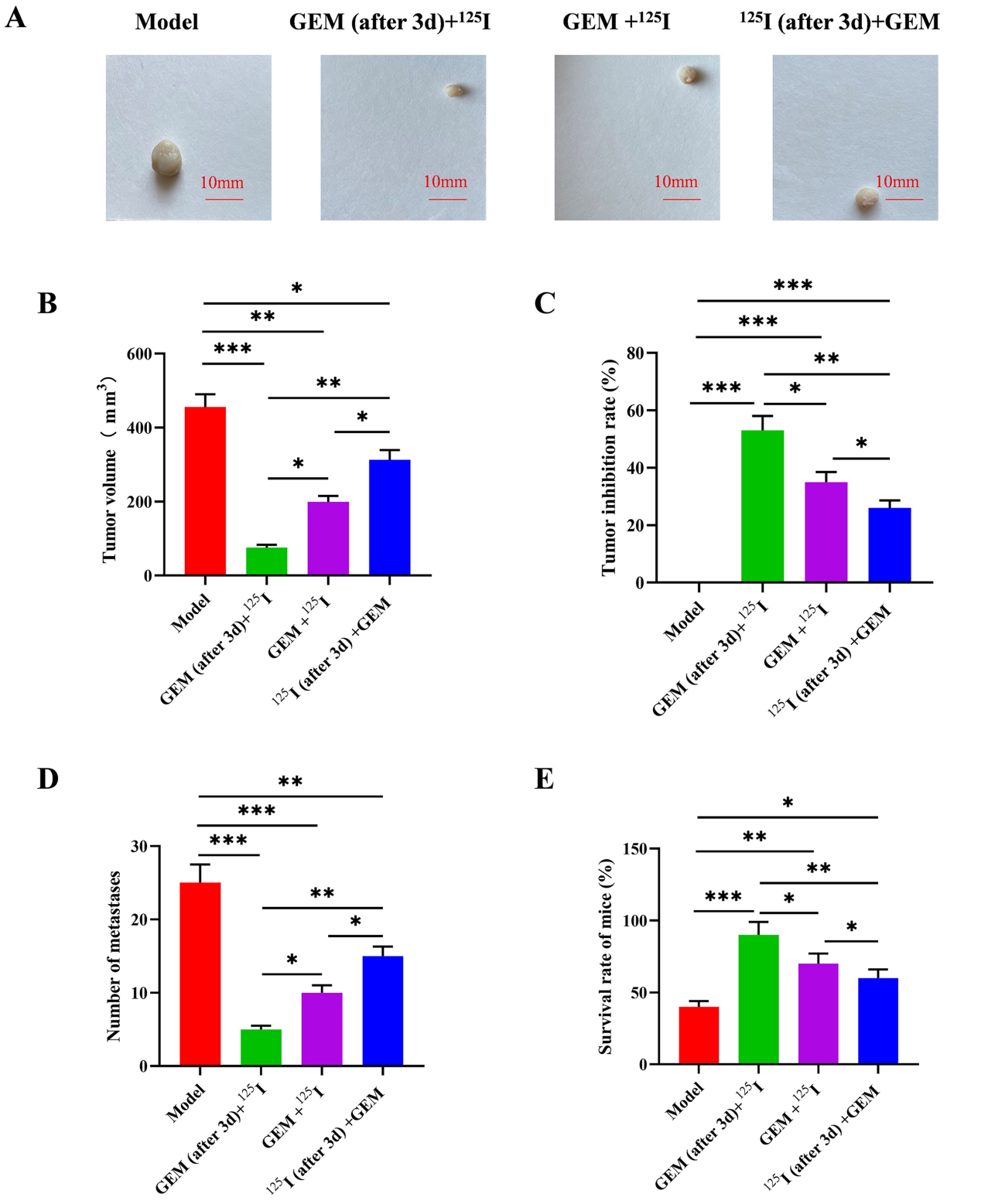

Fig. 2. Inhibitory effects of three different treatment strategies on pancreatic tumors. (A,B) Tumor Solid Images (A) and measurement of tumor volume (B). (C) The tumor inhibition rate was calculated. (D) Number of metastatic lesions. (E) Survival rate of mice at the end of the experiment (n = 10). (*$p < 0.05$, **$p < 0.01$, ***$p < 0.001$).

hibitory effect of ^{125}I seeds combined with GEM on PANC-1 cell proliferation was significantly better than that of ^{125}I seeds or GEM alone ($p < 0.05$, $p < 0.01$).

Fig. 1B illustrates the effect of ^{125}I seeds and GEM on apoptosis in PANC-1 cells. The results showed that the apoptosis rate of PANC-1 cells in the GEM (30 nM) treat-

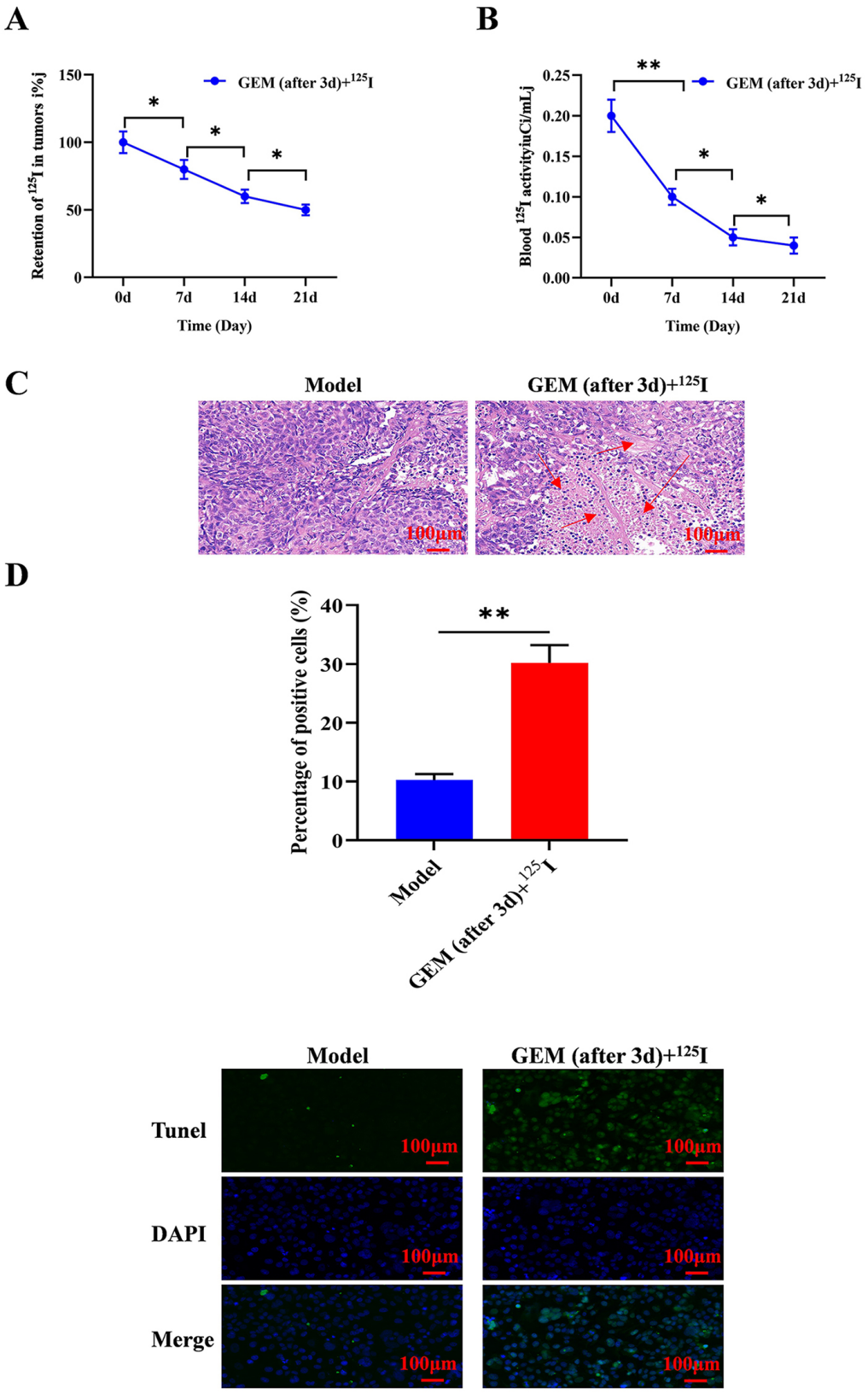

Fig. 3. Toxicity of GEM (after 3 d) + ^{125}I treatment on pancreatic tumor cells *in vivo*. (A) The amount of ^{125}I radiation in the tumor. (B) The amount of ^{125}I radioactivity in the blood. (C) The pathology of the pancreatic tumor tissue was evaluated by Hematoxylin and Eosin (HE) staining. The red arrows represent local necrotic and inflammatory regions. (D) The apoptosis of tumor cells was evaluated by Terminal deoxynucleotidyl transferase dUTP nick end labeling (TUNEL) staining (n = 10). Scale bar: 100 μm (*$p < 0.05$, **$p < 0.01$).

ment group, ^{125}I (6 Gy) treatment group, and GEM (30 nM) + ^{125}I (6 Gy) combined treatment group was significantly higher than that in the Control group ($p < 0.05$, $p < 0.01$, and $p < 0.001$). Compared with the GEM (30 nM) treatment group, ^{125}I (6 Gy) irradiation had a lower pro-apoptotic effect on PANC-1 cells ($p < 0.05$). Compared with the GEM (30 nM) treatment group and ^{125}I (6 Gy) treatment group, the apoptosis rate of PANC-1 cells in the GEM (30 nM) + ^{125}I (6 Gy) combined treatment group was significantly increased ($p < 0.01$, and $p < 0.001$).

Next, we determined the effects of ^{125}I seeds and GEM on mitochondrial membrane potential in PANC-1 cells. Under normal mitochondrial membrane potential conditions, JC-1 exists in an aggregated state, emitting red fluorescence. When the mitochondrial membrane potential decreases, JC-1 transitions from its aggregated state to a monomeric form, resulting in an increase in green fluorescence. Therefore, an increase in the JC-1 green fluorescence ratio reflects a decrease in mitochondrial membrane potential. The results are shown in Fig. 1C. Compared with the Control group, the mitochondrial membrane potential was significantly decreased in the GEM (30 nM) treatment group, ^{125}I (6 Gy) treatment group, and GEM (30 nM) + ^{125}I (6 Gy) combined treatment group ($p < 0.05$, $p < 0.01$, $p < 0.001$). When treated with ^{125}I seeds or GEM alone, the mitochondrial membrane potential of PANC-1 cells in the ^{125}I seed radiation group was higher than that in the GEM treatment group ($p < 0.05$). Compared to the GEM (30 nM) treatment group and ^{125}I (6 Gy) treatment group, the mitochondrial membrane potential of PC cells treated with the GEM (30 nM) + ^{125}I (6 Gy) combined treatment group was lower ($p < 0.05$, and $p < 0.01$).

The Therapeutic Effects of ^{125}I Brachytherapy and Gemcitabine were Evaluated in a PC Model

We evaluated the therapeutic effect of three different treatment strategies, ^{125}I brachytherapy, and GEM on PC tumors. The first strategy was to perform ^{125}I seed implantation surgery in mice 3 days after GEM treatment. The second strategy was to perform ^{125}I seed implantation surgery in mice at the same time as GEM treatment. The third strategy was to treat the mice with GEM three days after ^{125}I seed implantation surgery.

First, we determined the effect of the three treatment regimens on tumor volume. As shown in Fig. 2A,B, in PANC-1 xenograft mice, all treatment groups significantly inhibited tumor growth ($p < 0.05$). However, there were significant differences in tumor volume among groups ($p < 0.05$, and $p < 0.01$); the treatment effect of ^{125}I seed implantation after three days of GEM treatment was significantly better than that of the other two groups. Compared with the GEM (after 3 d) + ^{125}I group, tumor volume was distinctly higher in the GEM + ^{125}I treatment group and ^{125}I (after 3 d) + GEM treatment group ($p < 0.05$, and $p < 0.01$). In addition, the tumor inhibition rate of the GEM + ^{125}I treatment group and ^{125}I (after 3 d) + GEM treatment group was significantly lower than that of the GEM (after 3 d) + ^{125}I group ($p < 0.05$, and $p < 0.01$) (Fig. 2C).

We simultaneously evaluated the effect of the three treatment regimens on the number of metastatic lesions in mice. As shown in Fig. 2D, the number of metastatic lesions in the three treatment groups was significantly lower than that in the Model group ($p < 0.001$). There were significant differences in the number of metastatic lesions among the three treatment groups ($p < 0.05$, $p < 0.01$), and the number of metastatic lesions was the lowest in the GEM (after 3 d) + ^{125}I group.

We measured the survival rate of the mice after 21 days of treatment with the three regimens (Fig. 2E). Whereas the survival rate of mice in the Model group was approximately 40%, the survival rate of mice in all treatment groups was significantly higher. Compared to the other groups, the GEM (after 3 d) + ^{125}I group had the highest survival rate ($p < 0.05$, $p < 0.01$, and $p < 0.001$).

Based on the observation of the therapeutic effects of the three treatment regimens, we chose to perform ^{125}I seed implantation surgery in mice after 3 days of GEM treatment for subsequent experiments.

Effect of ^{125}I Brachytherapy Combined with Gemcitabine on the Cytotoxicity of Tumor Cells

During the study, we evaluated the radioactivity of ^{125}I in the tumor and blood of mice after GEM (after 3 d) + ^{125}I treatment (Fig. 3A,B). The results showed that the radioactive content of ^{125}I in the tumor and blood of mice decreased gradually with the extension of treatment time in a time-dependent manner ($p < 0.05$).

The effect of GEM (after 3 d) + ^{125}I treatment on mouse pancreatic tissue was evaluated by Hematoxylin and Eosin (HE) staining (Fig. 3C). There are marked areas of necrosis in untreated PC tissue (Model). After GEM (after 3 d) + ^{125}I treatment, the pancreatic tumor tissue showed localized necrosis, and more obvious interstitial fibrosis and inflammation.

Next, we performed histological analysis of tumor sections using TUNEL staining to see the effect on tumor cytotoxicity after combined treatment with GEM and ^{125}I. As shown in Fig. 3D, the tumor cells in the Model group were stained light, indicating that the number of apoptotic cells was the least. This indicated that GEM (after 3 d) + ^{125}I had induced obvious apoptosis of local tumor cells ($p < 0.01$).

^{125}I Brachytherapy Combined with Gemcitabine Reduced Related Enzyme Activities in the Blood

To explore the effect of ^{125}I brachytherapy combined with GEM on biochemical parameters in blood, serum levels of sPLA2, amylase, ALT, and AST were measured (Fig. 4A–D). Compared with the Control group, the activity levels of sPLA2, amylase, ALT, and AST were significantly

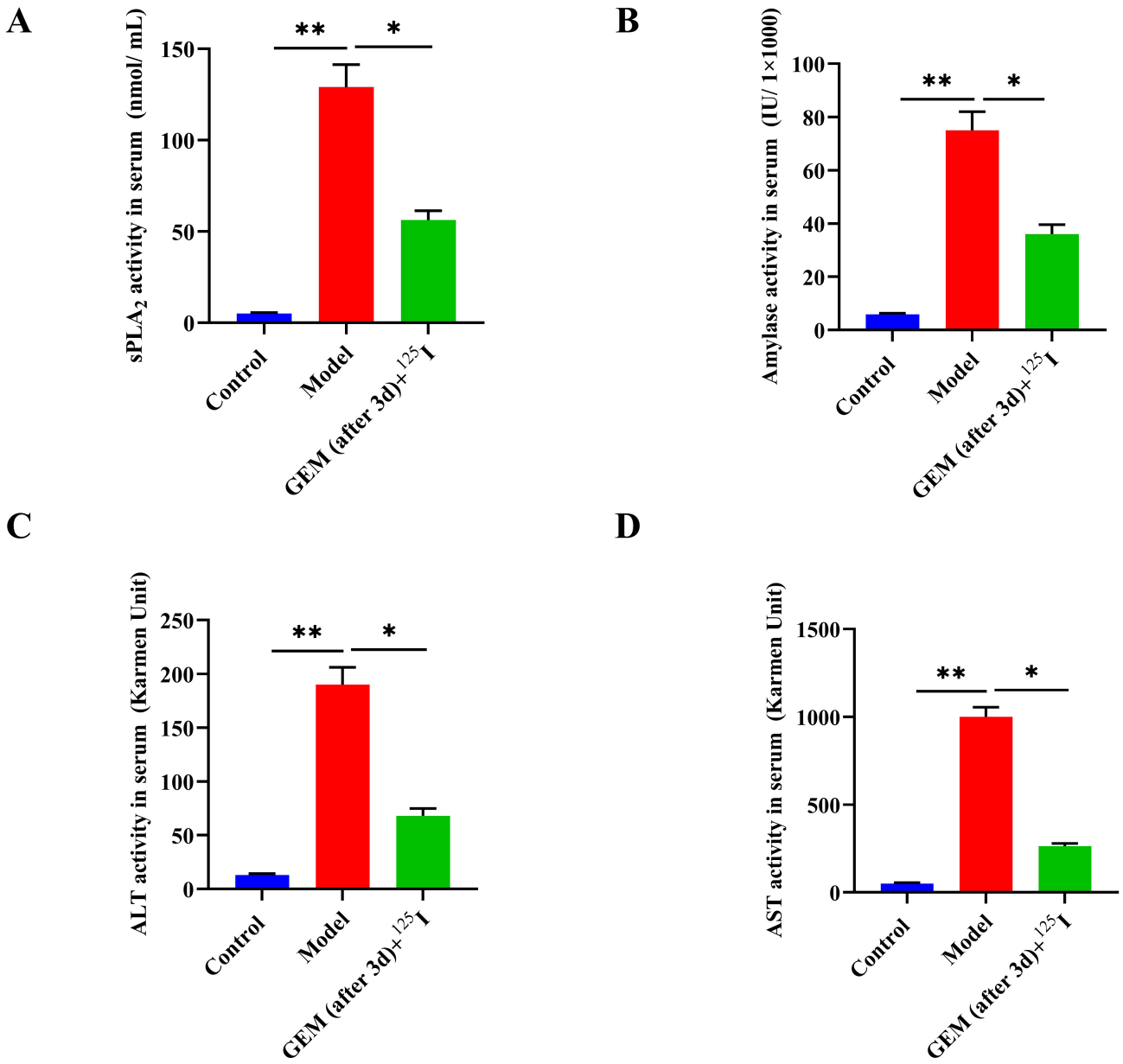

Fig. 4. Effect of GEM (after 3 d) + ^{125}I treatment on serum levels of sPLA2, amylase, ALT, and AST. (A) The level of sPLA2 in serum. (B) The level of amylase in serum. (C) The level of ALT in serum. (D) The level of AST in serum (n = 10). (*$p < 0.05$, **$p < 0.01$). sPLA2, secretory phospholipase A2; ALT, Alanine Aminotransferase; AST, Aspartate Aminotransferase.

increased in the Model group ($p < 0.01$). Compared with the Model group, ^{125}I brachytherapy combined with GEM significantly reduced the activity levels of sPLA2, amylase, ALT, and AST ($p < 0.05$) (Fig. 4A–D).

Effect of ^{125}I Brachytherapy Combined with Gemcitabine on Apoptosis-Related Proteins in Tumors

We determined the expression levels of Cleaved Caspase-3, Cleaved Caspase-9, Bax, and Bcl-2 in pancreatic tumor tissues to evaluate the impact of GEM and ^{125}I combination treatment on apoptosis pathways (Fig. 5A–D). The results showed that, compared to the Model group, the expression levels of Cleaved Caspase-3 and Cleaved Caspase-9, which are key markers of the activation of apoptosis, were significantly increased in the GEM (after 3 days) + ^{125}I group. This suggests enhanced activation of the caspase cascade, which is crucial for the execution phase of cell apoptosis. Additionally, the pro-apoptotic protein Bax was also significantly upregulated in the combination treatment group, indicating a shift towards the promotion of apoptosis. In contrast, the anti-apoptotic protein Bcl-2 was significantly downregulated in the same group ($p < 0.01$), further confirming the induction of apoptosis by the combination therapy. These changes in protein expression levels collectively suggest that GEM combined with ^{125}I treatment po-

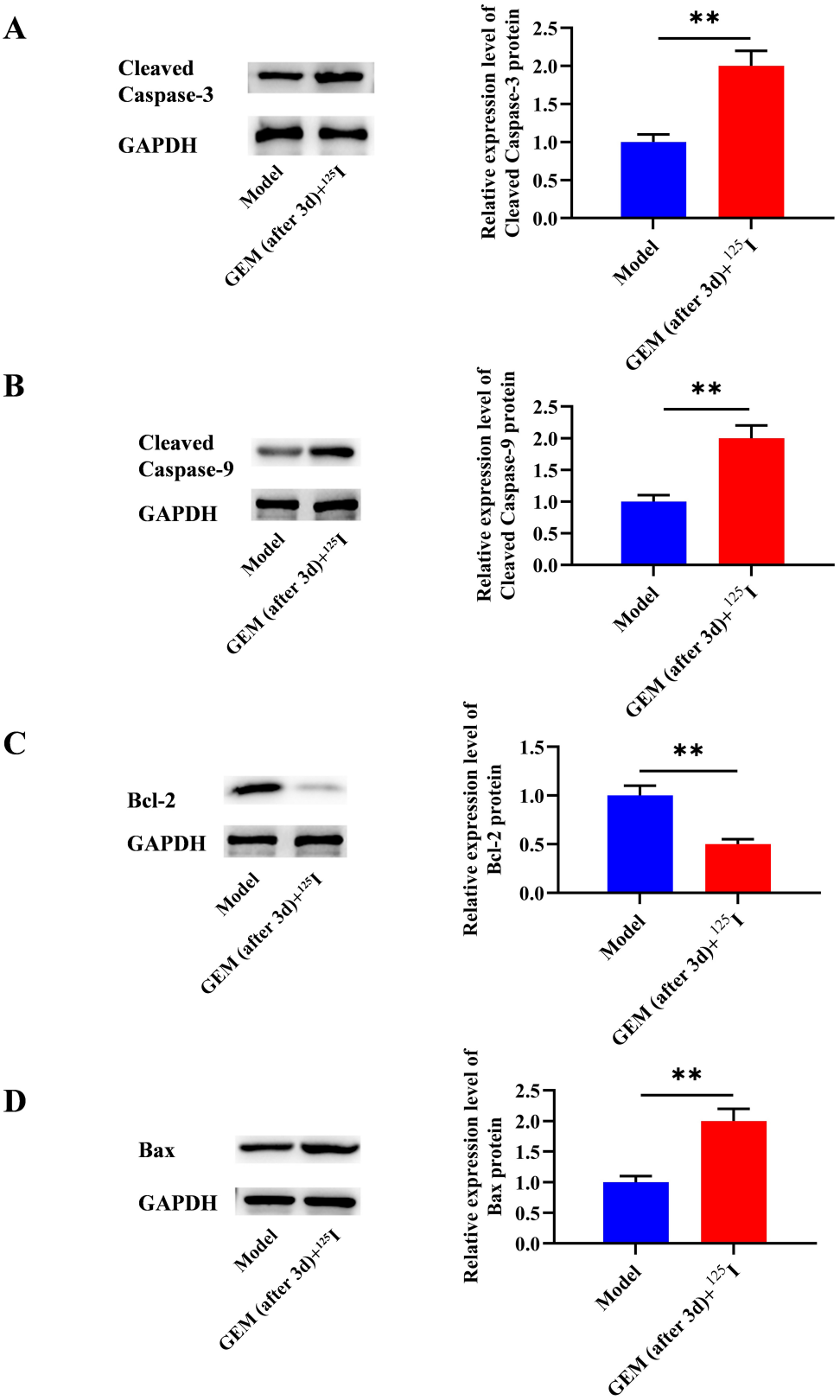

Fig. 5. Cleaved Caspase-3, Cleaved Caspase-9, Bax, and Bcl-2 protein expression in ^{125}I brachytherapy combined with gemcitabine treatment. (A) The level of Cleaved Caspase-3 protein. (B) The level of Cleaved Caspase-9 protein. (C) The level of Bcl-2 protein. (D) The level of Bax protein (n = 10). (**$p < 0.01$). GAPDH, Glyceraldehyde 3-phosphate dehydrogenase; Bcl-2, B-cell lymphoma 2; Bax, Bcl-2–associated X protein.

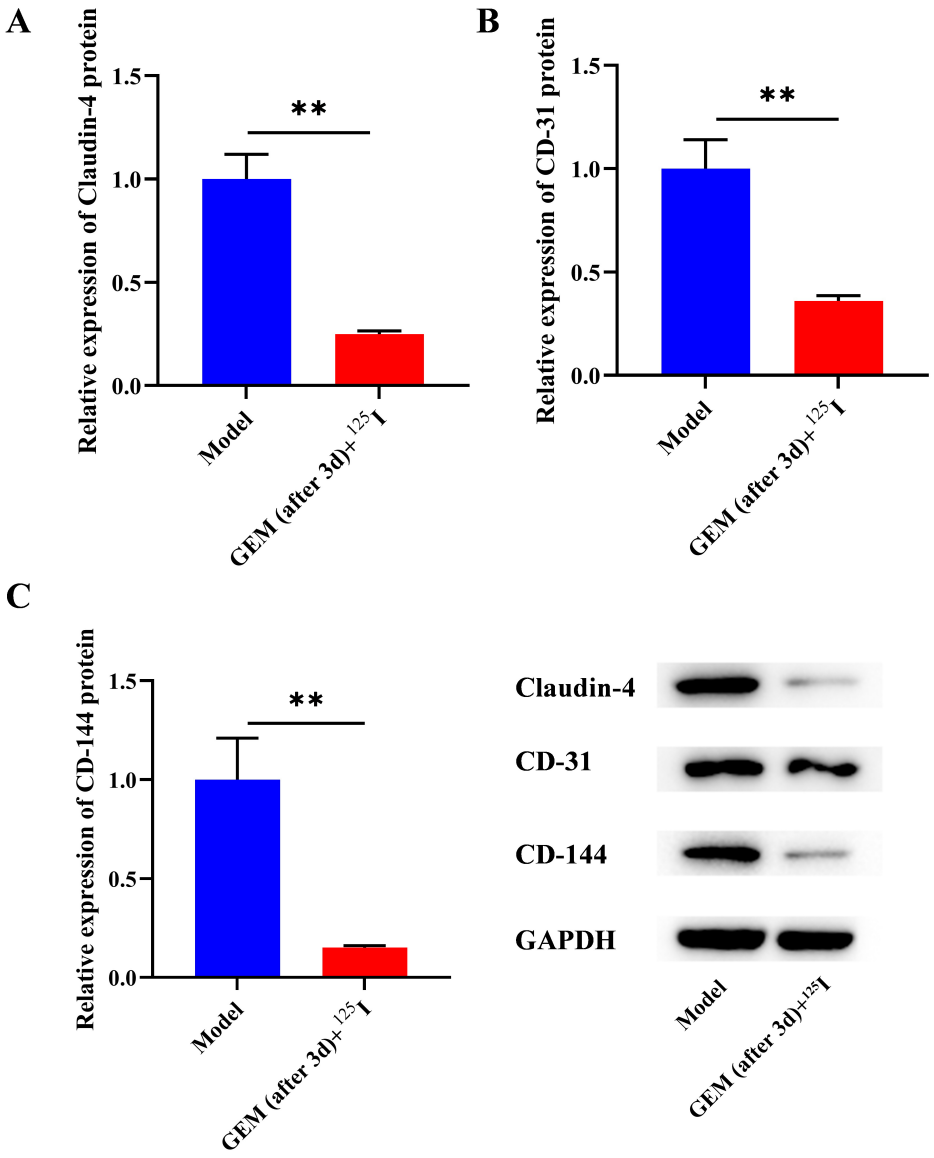

Fig. 6. Potential effects of ^{125}I and GEM on the tumor microenvironment of pancreatic tumors. (A–C) The protein expression levels of Claudin-4 (A), CD-31 (B) and CD-144 (C) in tumor tissues were determined by Western blot (n = 10) (**$p < 0.01$). CD-31, Cluster of Differentiation 31; CD-144, Cluster of Differentiation 144.

tentiates apoptotic mechanisms in pancreatic tumor tissues, thereby inhibiting tumor growth more effectively than either treatment alone (Fig. 5A–D).

Effect of ^{125}I Brachytherapy Combined with Gemcitabine on the Microenvironment of Pancreatic Tissue

Claudin-4, a protein that regulates the structure and function of tight junctions between cells, is present in PANC-1 pancreatic tumor cells. Claudin-4 expression was significantly reduced in tumor cells treated with GEM (after 3 d) + ^{125}I compared with the Model group ($p < 0.01$) (Fig. 6A).

CD-31, also known as platelet endothelial cell adhesion molecule, is upregulated by radiotherapy due to its role as a vascular marker [17]. The results indicated that the expression of CD-31 in the GEM (after 3 d) + ^{125}I treatment group was significantly reduced compared to that in the Model group ($p < 0.01$) (Fig. 6B).

CD-144 is a protein used to support the vascular endothelial barrier. After GEM (after 3 days) + ^{125}I treatment, the protein expression level of CD-144 in tumor cells was significantly lower than that in the Model group ($p < 0.01$) (Fig. 6C).

These expression changes in the tumor microenvironment suggest that the combination of ^{125}I brachytherapy and GEM treatment greatly attenuates the biological barrier that regulates tumor permeability.

Discussion

Radioactive particles have attracted interest in the treatment of solid tumors. In particular, radioactive seed implantation technology can selectively and continuously inject high concentrations of radioactive materials into tumors [18]. Our study shows that ^{125}I brachytherapy has a synergistic effect with GEM chemotherapy *in vitro*, and its efficacy is also present in an *in vivo* PC model.

It is well known that GEM is the first-line chemotherapy drug for the treatment of PC but it faces a major challenge due to chemoresistance [19]. Zhang *et al.* [20] showed that radiation doses greater than 3.12 Gy of ^{125}I seeds significantly reduced the viability of human neuroblastoma cells. Wang *et al.* [21] showed that ^{125}I seed radiation triggered apoptosis and autophagy by inducing increased production of reactive oxygen species in human esophageal squamous cell carcinoma cells. At the same time, the maximum cell death was observed when the radiation dose was 6 Gy [21]. This study showed that both ^{125}I brachytherapy and GEM alone inhibited the proliferation of PC cells, whereas the combination of ^{125}I brachytherapy and gemcitabine was superior to either alone. Our data also indicated that ^{125}I brachytherapy and gemcitabine treatment induced apoptosis in PANC-1 cells by inducing a decrease in mitochondrial membrane potential. Therefore, we hypothesized that ^{125}I brachytherapy could improve drug sensitivity in the synergistic treatment of PC.

A previous study has shown that different regimens of neoadjuvant radiotherapy based on GEM have significantly different efficacies in the treatment of PC [22]. Our data suggest that to maximize the synergy between systemic GEM therapy and brachytherapy, GEM should be administered for some time before combining ^{125}I radiotherapy. The levels of sPLA2, amylase, AST, and ALT in the blood can reflect the recovery of pancreatic function [23]. Performing ^{125}I seed implantation surgery 3 days after GEM treatment may capitalize on the sensitivity of tumor cells to GEM. This timing could potentially lead to a more pronounced effect of radioiodine implantation on tumors already influenced by GEM. There might be a synergistic effect between GEM and radioiodine implantation, enhancing each other's therapeutic effects. Conducting ^{125}I seed implantation surgery at a specific time point may enhance synergy with the effects of GEM. Tumor cells exhibit varying sensitivities to treatment at different points in the cell cycle. Performing ^{125}I seed implantation surgery 3 days after GEM treatment might align with a specific cell cycle phase, where tumor cells are particularly susceptible to the treatment. In our study, GEM (after 3 d) + ^{125}I treatment significantly reduced the levels of sPLA2, amylase, AST, and ALT, indicating that GEM (after 3 d) + ^{125}I treatment reduced systemic inflammatory response and organ failure. The process of apoptosis is tightly regulated by caspases and the Bcl-2 family. In this study, GEM (after 3 d) + ^{125}I induced apoptosis in tumor cells. It decreased the expression of apoptosis inhibitor protein Bcl-2 and increased the expression of pro-apoptotic protein Bax. It also induced the activation of Caspase-3 and Caspase-9, thereby promoting the apoptosis of PANC-1 cells. Sun *et al.* [24] demonstrated that hypericin can reduce the resistance of pancreatic tumor cells to GEM, and promote the apoptosis of Capan-2 cells by inhibiting the level of Bcl-2, stimulating the level of Bax and triggering the activation of caspases. The tumor microenvironment has long been the root cause of drug resistance in PC because the tumor microenvironment is composed of different non-tumor cells as well as abundant extracellular matrix components, with multiple biochemical and physical interactions between various cellular and cell-free components to promote tumor progression and treatment resistance [25]. Overcoming this barrier has been the focus of clinical research. Jia *et al.* [26] treated the tumor microenvironment with a nano delivery system that could alter the tumor microenvironment in PC by depleting the extracellular matrix, inhibiting associated fibrocytes to reverse immunosuppression, and promoting angiogenesis. Kang *et al.* [27] designed a novel non-steroidal vitamin D receptor modulator in combination with GEM to reshape the tumor microenvironment and effectively inhibit the activity of PC cells. Our findings indicate that ^{125}I brachytherapy enhances tumor permeability, resulting in elevated GEM accumulation. This heightened drug concentration sensitizes the tumor tissue to the cytotoxic effects of radiation. Consequently, the radiation induces tumor volume reduction, diminishes the microenvironment, and lowers connexin levels in the stroma. The enhanced permeability fosters increased GEM uptake during subsequent chemotherapy, establishing a positive feedback loop of synergistic therapy. This augmented permeability underscores the successful combination of ^{125}I with chemotherapeutic agents to achieve radiosensitization, microenvironment modulation, and direct contributions to cytotoxicity.

This study used a mouse model to evaluate therapeutic strategies for pancreatic cancer. Despite the important role of mouse models in preliminary screening and mechanistic studies, their biological characteristics may differ from human pancreatic cancer, thus limiting the direct applicability and generalization of the results. The treatment and observation period in this study were relatively short, especially with evaluation occurring only 3 days post-GEM treatment, which may not fully reflect long-term treatment effects and potential complications. Although *in vitro* experiments demonstrated the potential of combined GEM and ^{125}I therapy, translating these results to *in vivo* models and ultimately to clinical practice requires consideration of more complex biological variables and treatment response differences. This study focused on the combined effects of GEM and ^{125}I radioactive seed implantation therapy, restricting exploration of the general applicability of

other treatment modalities or combination therapies. While changes in tumor microenvironment and apoptosis-related proteins were assessed, the molecular mechanisms and signaling pathways of combined GEM and ^{125}I therapy were not deeply explored, which is crucial for understanding the exact mechanisms of synergistic effects and optimizing treatment strategies. Despite providing experimental data in mouse models, the clinical relevance and feasibility of this study require validation through further clinical research.

Conclusion

Despite the availability of well-developed chemoradiotherapy options, PC still displays a high recurrence rate and poor survival rate. Our results suggest that ^{125}I seed implantation performed 3 days after GEM administration has better efficacy in PC mice. It can promote tumor cell apoptosis and reduce tumor metastasis by reducing mitochondrial membrane potential, improving the tumor microenvironment, and reducing the systemic inflammatory response.

Availability of Data and Materials

The datasets used and/or analyzed during the current study are available from the corresponding author on reasonable request.

Author Contributions

QL and YL contributed to the concept and designed the research study. JL and XH performed the research. ZL and YL provided help and advice on the experiments. JL and ZL contributed to the analysis and interpretation of the data. QL and XH drafted the manuscript. All authors contributed to the important editorial changes in the manuscript. All authors read and approved the final manuscript. All authors participated sufficiently in the work to take public responsibility for appropriate portions of the content and agreed to be accountable for all aspects of the work in ensuring that questions related to its accuracy or integrity.

Ethics Approval and Consent to Participate

The study has obtained approval from the Beijing KeWeiTe for Experimental Animal Welfare Ethics Committee (Approval No. KWT-2023-084).

Acknowledgment

Not applicable.

Funding

This research was funded by the Clinical Research Special Support Fund of Wu Jieping Medical Foundation. (No. 320.6750.2021-22-12).

Conflict of Interest

The authors declare no conflict of interest.

References

[1] Siegel RL, Miller KD, Wagle NS, Jemal A. Cancer statistics, 2023. CA: a Cancer Journal for Clinicians. 2023; 73: 17–48.

[2] Jiang H, Liu X, Knolhoff BL, Hegde S, Lee KB, Jiang H, *et al*. Development of resistance to FAK inhibition in pancreatic cancer is linked to stromal depletion. Gut. 2020; 69: 122–132.

[3] Kolbeinsson HM, Chandana S, Wright GP, Chung M. Pancreatic Cancer: A Review of Current Treatment and Novel Therapies. Journal of Investigative Surgery: the Official Journal of the Academy of Surgical Research. 2023; 36: 2129884.

[4] Bailey P, Chang DK, Nones K, Johns AL, Patch AM, Gingras MC, *et al*. Genomic analyses identify molecular subtypes of pancreatic cancer. Nature. 2016; 531: 47–52.

[5] Ren B, Cui M, Yang G, Wang H, Feng M, You L, *et al*. Tumor microenvironment participates in metastasis of pancreatic cancer. Molecular Cancer. 2018; 17: 108.

[6] Ho WJ, Jaffee EM, Zheng L. The tumour microenvironment in pancreatic cancer - clinical challenges and opportunities. Nature Reviews. Clinical Oncology. 2020; 17: 527–540.

[7] Neoptolemos JP, Palmer DH, Ghaneh P, Psarelli EE, Valle JW, Halloran CM, *et al*. Comparison of adjuvant gemcitabine and capecitabine with gemcitabine monotherapy in patients with resected pancreatic cancer (ESPAC-4): a multicentre, open-label, randomised, phase 3 trial. Lancet (London, England). 2017; 389: 1011–1024.

[8] Regine WF, Winter KA, Abrams R, Safran H, Hoffman JP, Konski A, *et al*. Fluorouracil-based chemoradiation with either gemcitabine or fluorouracil chemotherapy after resection of pancreatic adenocarcinoma: 5-year analysis of the U.S. Intergroup/RTOG 9704 phase III trial. Annals of Surgical Oncology. 2011; 18: 1319–1326.

[9] Daly MB, Pal T, Berry MP, Buys SS, Dickson P, Domchek SM, *et al*. Genetic/Familial High-Risk Assessment: Breast, Ovarian, and Pancreatic, Version 2.2021, NCCN Clinical Practice Guidelines in Oncology. Journal of the National Comprehensive Cancer Network: JNCCN. 2021; 19: 77–102.

[10] Motoi F, Kosuge T, Ueno H, Yamaue H, Satoi S, Sho M, *et al*. Randomized phase II/III trial of neoadjuvant chemotherapy with gemcitabine and S-1 versus upfront surgery for resectable pancreatic cancer (Prep-02/JSAP05). Japanese Journal of Clinical Oncology. 2019; 49: 190–194.

[11] Jia SN, Wen FX, Gong TT, Li X, Wang HJ, Sun YM, *et al*. A review on the efficacy and safety of iodine-125 seed implantation in unresectable pancreatic cancers. International Journal of Radiation Biology. 2020; 96: 383–389.

[12] Li D, Jia YM, Cao PK, Wang W, Liu B, Li YL. Combined effect of ^{125}I and gemcitabine on PANC-1 cells: Cellular apoptosis and cell cycle arrest. Journal of Cancer Research and Therapeutics. 2018; 14: 1476–1481.

[13] Benchimol A, Marsh CA, Desser KB. Discordant left ventricular pressure and apexcardiographic pulsus alternans. Chest. 1975; 67: 477–479.

[14] Verhoeff JJC, Stalpers LJA, Coumou AW, Koedooder K, Lavini

C, Van Noorden CJF, *et al*. Experimental iodine-125 seed irradiation of intracerebral brain tumors in nude mice. Radiation Oncology (London, England). 2007; 2: 38.

[15] Wang ZM, Lu J, Zhang LY, Lin XZ, Chen KM, Chen ZJ, *et al*. Biological effects of low-dose-rate irradiation of pancreatic carcinoma cells in vitro using 125I seeds. World Journal of Gastroenterology. 2015; 21: 2336–2342.

[16] Lu J, Wu XJ, Hassouna A, Wang KS, Li Y, Feng T, *et al*. Gemcitabine fucoxanthin combination in human pancreatic cancer cells. Biomedical Reports. 2023; 19: 46.

[17] Quarmby S, Kumar P, Wang J, Macro JA, Hutchinson JJ, Hunter RD, *et al*. Irradiation induces upregulation of CD31 in human endothelial cells. Arteriosclerosis, Thrombosis, and Vascular Biology. 1999; 19: 588–597.

[18] Wang Y, Kang P, He W, Li R. MR-guided 125I seed implantation treatment for maxillofacial malignant tumor. Journal of Applied Clinical Medical Physics. 2021; 22: 92–99.

[19] Sarvepalli D, Rashid MU, Rahman AU, Ullah W, Hussain I, Hasan B, *et al*. Gemcitabine: A Review of Chemoresistance in Pancreatic Cancer. Critical Reviews in Oncogenesis. 2019; 24: 199–212.

[20] Zhang D, Xu H, Wang Y, Wang K, Wang Y, Wu B, *et al*. 125I radiation downregulates TRPV1 expression through miR 1246 in neuroblastoma cells. Oncology Reports. 2019; 42: 243–252.

[21] Wang C, Li TK, Zeng CH, Fan R, Wang Y, Zhu GY, *et al*. Iodine 125 seed radiation induces ROS mediated apoptosis, autophagy and paraptosis in human esophageal squamous cell carcinoma cells. Oncology Reports. 2020; 43: 2028–2044.

[22] Janssen QP, van Dam JL, Bonsing BA, Bos H, Bosscha KP, Coene PPLO, *et al*. Total neoadjuvant FOLFIRINOX versus neoadjuvant gemcitabine-based chemoradiotherapy and adjuvant gemcitabine for resectable and borderline resectable pancreatic cancer (PREOPANC-2 trial): study protocol for a nationwide multicenter randomized controlled trial. BMC Cancer. 2021; 21: 300.

[23] Tomita Y, Kuwabara K, Furue S, Tanaka K, Yamada K, Ueno M, *et al*. Effect of a selective inhibitor of secretory phospholipase A2, S-5920/LY315920Na, on experimental acute pancreatitis in rats. Journal of Pharmacological Sciences. 2004; 96: 144–154.

[24] Sun L, Shang H, Wu Y, Xin X. Hypericin-mediated photodynamic therapy enhances gemcitabine induced Capan-2 cell apoptosis via inhibiting NADPH level. The Journal of Pharmacy and Pharmacology. 2022; 74: 596–604.

[25] Hessmann E, Buchholz SM, Demir IE, Singh SK, Gress TM, Ellenrieder V, *et al*. Microenvironmental Determinants of Pancreatic Cancer. Physiological Reviews. 2020; 100: 1707–1751.

[26] Jia M, Zhang D, Zhang C, Li C. Nanoparticle-based delivery systems modulate the tumor microenvironment in pancreatic cancer for enhanced therapy. Journal of Nanobiotechnology. 2021; 19: 384.

[27] Kang Z, Wang C, Tong Y, Li Y, Gao Y, Hou S, *et al*. Novel Non-secosteroidal Vitamin D Receptor Modulator Combined with Gemcitabine Enhances Pancreatic Cancer Therapy through Remodeling of the Tumor Microenvironment. Journal of Medicinal Chemistry. 2021; 64: 629–643.